

---

This is an electronic reprint of the original article.  
This reprint may differ from the original in pagination and typographic detail.

Vuyyuru, Sravan K.R.; Valkonen, Risto; Kwon, Do Hoon; Tretyakov, Sergei A.  
**Array Scattering Synthesis for Anomalous Deflection Using Passive Aperiodic Loadings**

*Published in:*  
18th European Conference on Antennas and Propagation, EuCAP 2024

*DOI:*  
[10.23919/EuCAP60739.2024.10501038](https://doi.org/10.23919/EuCAP60739.2024.10501038)

Published: 01/01/2024

*Document Version*  
Publisher's PDF, also known as Version of record

*Please cite the original version:*  
Vuyyuru, S. K. R., Valkonen, R., Kwon, D. H., & Tretyakov, S. A. (2024). Array Scattering Synthesis for Anomalous Deflection Using Passive Aperiodic Loadings. In *18th European Conference on Antennas and Propagation, EuCAP 2024* IEEE. <https://doi.org/10.23919/EuCAP60739.2024.10501038>

---

This material is protected by copyright and other intellectual property rights, and duplication or sale of all or part of any of the repository collections is not permitted, except that material may be duplicated by you for your research use or educational purposes in electronic or print form. You must obtain permission for any other use. Electronic or print copies may not be offered, whether for sale or otherwise to anyone who is not an authorised user.

# Array Scattering Synthesis for Anomalous Deflection Using Passive Aperiodic Loadings

Sravan K. R. Vuyyuru<sup>\*†</sup>, Risto Valkonen<sup>\*</sup>, Do-Hoon Kwon<sup>‡</sup>, and Sergei A. Tretyakov<sup>†</sup>

<sup>\*</sup> Nokia Bell Labs, Karakaari 7, 02610 Espoo, Finland

<sup>†</sup> Department of Electronics and Nanoengineering, School of Electrical Engineering, Aalto University, 02150 Espoo, Finland

<sup>‡</sup> Department of Electrical and Computer Engineering, University of Massachusetts Amherst, Amherst, MA 01003, USA

<sup>\*</sup>sravan.vuyyuru@nokia.com

**Abstract**—Large-scale anomalous reflectors in reconfigurable intelligent surface applications require a scanning capability to deflect the beam to an arbitrary angle without incurring parasitic scattering. In this study, we propose a design methodology for linear loaded antenna arrays by synthesizing the scattering characteristics with respect to impedance loads to attain perfect anomalous reflection. It relies on accurate prediction of the induced element port currents and their associated scattering behavior for any given set of load impedances. We develop a linear array with a fixed half wavelength spacing for scanning into extreme deflection angles. Using continuous and discretized load reactances, the tunability prospect of high-efficiency anomalous reflection is demonstrated.

**Index Terms**—Anomalous reflector, reconfigurable intelligent surface (RIS), receiving antennas, far-field scattering, aperiodic loadings.

## I. INTRODUCTION

During the past few years, reconfigurable intelligent surfaces (RISs) have emerged as potential tools for wavefront manipulation, aiming for versatile functionalities [1]. In particular, one of the extensively researched capabilities of RISs is anomalous reflection, as illustrated in Fig. 1. In these perfect anomalous reflectors, the reflected wave direction deviates from the conventional reflection law, whereby the incident angle  $\theta^i$  does not equal the reflection angle  $\theta^r$ . A simple approach in realizing anomalous reflection is using phase-gradient reflectors [2], [3], where each meta-atom is designed to control the local reflection coefficient. However, the power efficiency of anomalous reflection using linear phase-gradient reflectors diminishes gradually for large transformations of the wave propagation direction, predominantly attributed to the impedance mismatch and interference between the incident and reflected plane waves. Accompanied are strong parasitic reflections in undesired directions [4], [5]. On the other hand, advanced methods to achieve high-efficiency, wide-angle anomalous reflection employing periodic metasurfaces [4]–[6] and metagratings [7] have been proposed for diverse applications. However, research on modeling and designing highly directive and efficient anomalous reflectors of realizing *continuous* scanning of the deflection angle is at an early stage.

Continuous scanning of reflection angles proves impractical with periodic anomalous reflectors due to the dependency of the supercell period on the angles of incidence and reflection. Consequently, a periodic design requires a modification of

the array period for each deflection angle. However, this difficulty has been mitigated by employing reflectarrays characterized by a fixed geometrical period, typically  $\lambda/2$  ( $\lambda$  = free-space wavelength). Using the conventional reflectarray design approach [2], [3], the power efficiency will diminish gradually for large deflection angles (i.e., considerably larger than  $50^\circ$  for the case of normal incidence) due to unwanted parasitic reflections, similarly to the case of periodic metasurfaces [4], [5]. Based on scattering synthesis for infinite periodic loaded arrays [5], a novel approach for designing wide-angle anomalous reflectors has been demonstrated, which eliminates the need for supercell-level computation-intensive full-wave electromagnetic (EM) simulations. However, that design technique is limited to infinite periodic reflectors. In this work, we address the challenges of realizing continuous scanning of the deflection angle without compromising performance with a fixed structure of finite dimensions.

## II. PRINCIPLE AND METHODOLOGY

Figure 1 depicts anomalous deflection of an incident wave towards specific, non-specular extreme angles. Let us consider a finite array of metallic patches, each loaded with lumped elements and etched onto a dielectric substrate at a height  $h$  above a finite perfect electric conductor (PEC) ground plane. The spacing between the radiating elements is  $d = \lambda/2$ , allowing for scanning in the  $xz$ -plane.

Let us consider a configuration involving a receiving and scattering antenna, where the scattering characteristic of a load-terminated antenna depends on the load attached to its terminals [8]. The total scattered  $E$ -field,  $\mathbf{E}^s$ , scattered by an antenna with a load impedance  $Z_L$ , is determined by the combined contributions of zero-current scattering and port-current scattering [9] as

$$\mathbf{E}^s(Z_L) = \mathbf{E}^s(Z_L = \infty) - I_L \mathbf{E}_I, \quad (1)$$

where  $\mathbf{E}_I$  represents the radiated  $E$ -field in the transmitting (TX) mode for a unit input current excitation,  $\mathbf{E}^s(Z_L = \infty)$  denotes the scattered  $E$ -field in the receiving (RX) mode when its feed point is open-circuited, and  $I_L$  signifies the load current. Alternative decompositions of the same overall scattered field are available in the literature [9], [10].

The linearity relation of the scattered field decomposition (1) extends to the general RX antenna array with aperiodic

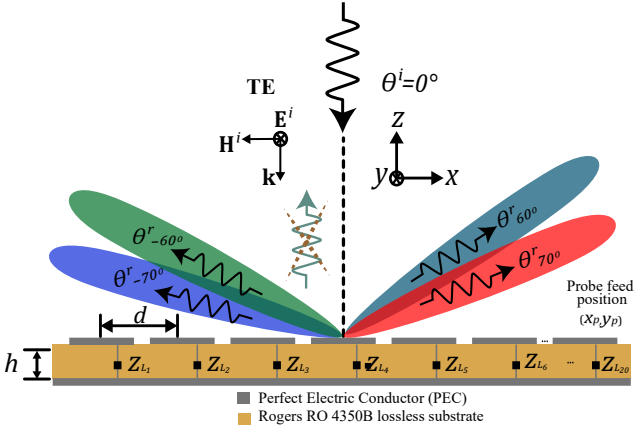


Fig. 1: Side view of a linear array under a normally incident plane wave illumination. The desired large deflection angles are  $\pm 60^\circ$  and  $\pm 70^\circ$ .

loadings. A spherical-wave variant of the plane-wave synthesis technique for infinite periodic arrays [5] is employed to engineer a finite-sized anomalous reflector. In an array comprising  $N$  loaded elements, a complex load  $Z_{Ln}$  ( $n = 1, \dots, N$ ) terminates the  $n$ -th element. In this paper, we emphasize that synthesis of scattering arrays based on (1) is applicable for arbitrary incident wave scenarios and antenna array configurations.

Throughout this paper, we assume that the linear antenna array is parallel with the  $x$ -axis and excited by a transverse electric (TE) polarized incident plane wave with an  $E$ -field

$$\mathbf{E}^i = \hat{y} E_0^i e^{-jk(x \sin \theta^i + z \cos \theta^i)}, \quad (2)$$

where  $\theta^i$  is the angle of incidence, and  $k$  is the free-space wavenumber. An  $e^{j\omega t}$  harmonic time dependence is assumed and suppressed. Reciprocity establishes a relationship between the parameters of the RX and TX modes when scanning in the direction  $(\theta^s, \phi^s) = (\pi - \theta^i, \phi^i - \pi)$ .

Extending the theory of an isolated RX antenna to an  $N$ -loaded RX antenna array, the open-circuit voltage and the load current expressions across the terminals take the vector form

$$\mathbf{V}_{oc} = \mathbf{h}(\theta^s, \phi^s) \cdot \mathbf{E}^i(O), \quad (3)$$

$$\mathbf{I}_L = (\mathbf{Z}_A + \mathbf{Z}_L)^{-1} \mathbf{V}_{oc}, \quad (4)$$

where  $\mathbf{Z}_A$  is the  $N \times N$  impedance matrix of the  $N$ -port antenna array. The full matrix  $\mathbf{Z}_A$  contains the self-impedances (diagonal positions) and mutual impedances (off-diagonal positions) of array elements, accounting for interactions between them.  $\mathbf{Z}_L$  is a diagonal matrix with load impedances  $Z_{Ln}$  at each port ( $n = 1, \dots, N$ ) of the  $N$ -port network. The column vector  $\mathbf{h}(\theta^s, \phi^s)$  of size  $N \times 1$  encompasses the vector effective heights for each individual element, calculated in the TX mode for specific scan angles  $(\theta^s, \phi^s)$ . The  $N \times 1$  column vector  $\mathbf{V}_{oc}$  collects all open-circuit voltages at the terminals of the RX antenna array. The column vector  $\mathbf{I}_L$  contains all individual load currents  $I_{Ln}$  ( $n = 1, \dots, N$ ) at the antenna array ports.

Conducting a series of preliminary electromagnetic (EM) simulations is necessary to enable algebraic global optimization of  $Z_{Ln}$  to achieve a scattered beam in an anomalous

direction. The matrix  $\mathbf{Z}_A$  and the vector  $\mathbf{h}(\theta^s)$  are computed using a TX full-wave EM simulation. Similarly,  $\mathbf{E}^s(\mathbf{Z}_L = \infty)$  is found using an RX simulation. Once the pre-computed matrices are obtained, we execute algebraic optimizations to synthesize arrays with the desired scattering characteristics. It is noteworthy to highlight that modifications in the incident wave direction or polarization requires new assessments of  $\mathbf{E}^s(\mathbf{Z}_L = \infty)$  only.

In the far-field region of the scattering array in a direction  $(\theta^r, \phi^r)$ , Eq. (1) for the total scattered  $E$ -field can be written as

$$\mathbf{E}^s(\mathbf{Z}_L) = \mathbf{E}^s(\mathbf{Z}_L = \infty) - \sum_{n=1}^N \frac{jk\eta I_{Ln}}{4\pi} \mathbf{h}_n(\theta^r, \phi^r) \frac{e^{-jkr}}{r}, \quad (5)$$

where  $\mathbf{h}_n(\theta^r, \phi^r)$  and  $I_{Ln}$  are the vector effective height and the load port current of the  $n$ -th port, respectively.  $\eta$  represents the free-space intrinsic impedance. In our approach to scattering synthesis, we adopt the bistatic scattering cross-section (SCS)  $\sigma$  [8]

$$\sigma(\mathbf{Z}_L, \theta^r) = \lim_{r \rightarrow \infty} 4\pi r^2 \frac{|\mathbf{E}^s(\mathbf{Z}_L)|^2}{|\mathbf{E}^i(O)|^2} \quad (6)$$

as a metric of the scattering intensity in the desired direction.

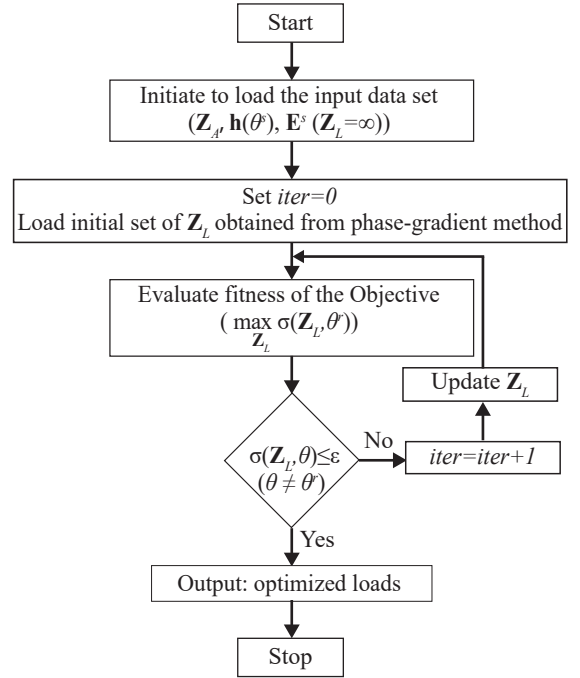


Fig. 2: Flow chart for the proposed algebraic optimization algorithm implemented in the MATLAB program.

We employ only passive load components to optimize the induced currents to achieve efficient anomalous reflection. The optimization process is performed by maximizing  $\sigma(\mathbf{Z}_L)$  in the desired direction by a meticulous tuning of  $Z_{Ln}$  ( $n = 1, \dots, N$ ). The algorithm revolves around individual variations of each reactive load, resulting in an algebraic

TABLE I: Summary of the optimized load reactances.

Deflection angle $\theta^r$ ( $^\circ$ )	Continuous optimized load reactances ( $\Omega$ )	SSL (dB)
$60^\circ$	28, 190, 15, 77, 5, 70, -15, 61, -52, 6, 88, -19, 46, 11921, 24, 441, 6, 58, 14, -1905	-11.7
$70^\circ$	-90, 39, -49, 30, -128, 51, 139, 16, 87, 29, 87, 20, 52, 22, 108, 14, 60, 10, 45, -34	-9.7
$-60^\circ$	-1905, 14, 58, 6, 441, 24, 11921, 46, -19, 88, 6, -52, 61, -15, 70, 5, 77, 15, 190, 28	-11.7
$-70^\circ$	-34, 45, 10, 60, 14, 108, 22, 52, 20, 87, 29, 87, 16, 139, 51, -128, 30, -49, 39, -90	-9.7

optimization across the entirety of the array. This synthesis strategy allows precise tailoring of the antenna scattering behavior in redirecting all the incident power from any angle into any desired direction.

To ensure precision of our results, we add constraints identified through numerical simulation analysis. The constraints are required to minimize unwanted deflections in the specular direction and other side-lobes, thereby contributing to enhancement of scattering in the desired direction. Both the fitness and cost functions formulate a multi-objective optimization problem toward finding the global optimal solution.

A visual representation of the multi-objective optimization process is shown in Fig. 2. Here, the parameter  $\epsilon$  represents a small positive constant. The optimization is performed using the *fmincon* function as a reliable and practical tool for multi-objective optimization in MATLAB. First, an initial set of load impedances is obtained from the conventional phase-gradient method to initiate the optimization process. Subsequently, we compute the bistatic SCS using (6) across the  $\theta^r$  range. The above step is iteratively executed by updating purely reactive impedance loads until the termination criterion is satisfied. This methodical approach ensures a systematic convergence towards the desired outcome. Finally, we compute the far-field bistatic SCS pattern for the optimized loads.

### III. OPTIMIZED FINITE PATCH ARRAYS FOR CONTINUOUS SCANNING

In this section, we demonstrate the optimization performance of finite anomalous reflector designs achieved through arithmetic optimization of aperiodic passive loadings. Specifically, we engineer a linear array characterized by a spacing of  $\lambda/2$ , tailored for TE-polarized incident plane waves, as illustrated in Fig. 1.

We begin our investigation by determining the dimensions of the single element, which is a self-resonant patch under periodic boundary conditions. The simulations are numerically analyzed using CST MICROWAVE STUDIO simulator. We use a linearly polarized PEC square patch antenna tuned for impedance match to  $50 \Omega$  at 28 GHz. We use Rogers RO4350B (lossless) substrate with a relative permittivity  $\epsilon_r = 3.66$  having a 0.338 mm thickness. The square patch dimension is 2.554 mm ( $0.2385\lambda$ ), and the feed position  $(x_p, y_p) = (0, 0.444)$  mm is optimized for impedance match to a  $50 \Omega$  load impedance at the desired frequency. The overall patch antenna array spans  $107 \text{ mm} \times 5.3534 \text{ mm}$  ( $10\lambda \times 0.5\lambda$ ) with a half-wavelength element spacing comprising 20 individual patch elements.

Figure 1 illustrates the desired deflection of a normally incident plane wave  $[(\theta^i, \phi^i) = (0, 0)]$  into  $[(\theta^r, \phi^r) = (\pm 60^\circ, 0)]$

and  $(\pm 70^\circ, 0)]$  in TE polarization. Since all probes on the patches have no  $x$ -displacement (i.e.,  $x_p = 0$ ) from the patch center, scattering in the positive and negative ranges of  $\theta^r$  occurs in a strictly mirror symmetric fashion. We do not consider deflection angles smaller than  $60^\circ$  since they are realized efficiently using the conventional linear phase gradient method. For infinite periodical arrays, reflections from  $\theta^i = 0^\circ$  to  $\theta^r = \pm 60^\circ$  and  $\pm 70^\circ$  directions require supercell periods of  $\lambda/\sin \theta^r \approx 1.1547\lambda$  and  $1.0642\lambda$ , respectively. These periods are obviously not divisible by  $\lambda/2$ , but we will demonstrate that the developed optimization method enables continuous scanning across all anomalous reflection directions using aperiodic finite array designs.

In addition to optimization of continuously varying load reactances, we draw a comparison between continuous load optimization and conventional linear phase-gradient method to assess the effectiveness of our proposed technique of the array design. We extended our comparison to quantized load optimization from 1 to 5-bit resolution, because using a wide range of continuously tunable load values may be not feasible in practice. To this end, we limit the allowed load values to a 1 ( $180^\circ$ ), 2 ( $90^\circ$ ), 3 ( $45^\circ$ ), 4 ( $22.5^\circ$ ), and 5 ( $11.25^\circ$ ) bit quantization resolution for realizing 2, 4, 8, 16, and 32 equally-spaced distinct reflection phase values at the load (phase increments in parentheses), respectively. This approach explores the precision and feasibility in real-world applications when digital phase shifters are employed. The optimized load reactance values and their corresponding CST simulated side-lobe levels (SLL), which account for the strongest unwanted scattering direction compared to the desired scattering direction, are reported in Table I.

Figure 3 also depicts the CST simulated results comparing between optimized continuous loads and phase gradient loads. The reported outcomes for continuous load values show a dominant scattering beam in the desired direction with minimized unwanted scattering. Although we aim to achieve scattering towards a specific desired angle, the scattering peak is not aligned precisely with the intended angle. A beam pointing error of  $3^\circ$  for  $\pm 70^\circ$  and  $2^\circ$  for  $\pm 60^\circ$  design are observed. This deviation arises from the constraints imposed by the finite number of individual patch-loaded elements and the coarse half-wave patch spacing in the antenna array. The outcomes of continuous load optimizations have favorable SSLs compared to phase gradient results.

The aperiodic distribution behavior of the induced load currents at the patch antenna terminals obtained from numerical simulations for continuous and phase gradient loads are plotted in Fig. 4 to compare the optimized current profile with the ideal linear phase gradient distribution. It is important

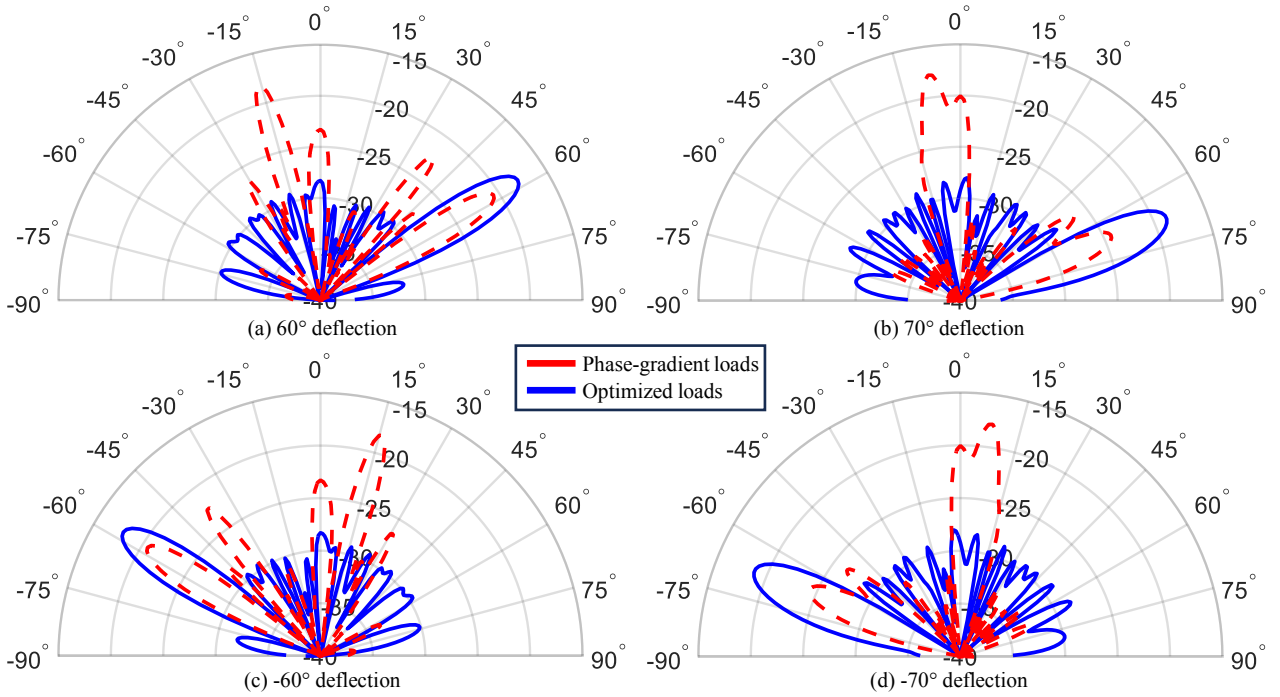


Fig. 3: CST-simulated bistatic SCS patterns (dBsm scale) of the anomalous reflector designs in the  $xz$ -plane, comparing phase-gradient method (red dashed line) and continuous load optimization (blue solid line). These figures represent the  $xz$ -plane ( $\phi = 0$ ) cut of the bistatic SCS for (a)  $60^\circ$ , (b)  $70^\circ$ , (c)  $-60^\circ$ , and (d)  $-70^\circ$  designs of the linear array of the anomalous reflector with a  $\lambda/2$  element spacing.

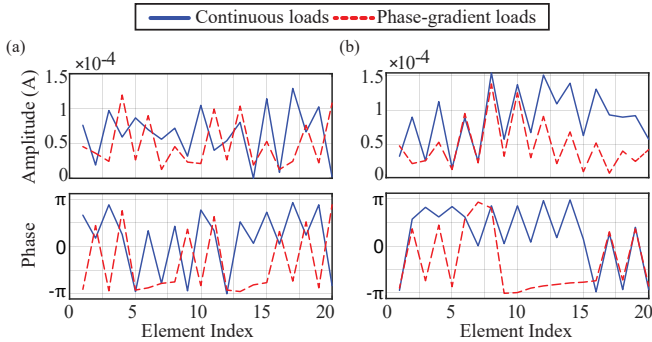


Fig. 4: CST-simulated amplitude and phase of the current distribution flowing at the patch antenna terminals to manipulate the reflected wavefronts, comparing continuous (blue solid line) and phase gradient (red dashed line) load outcomes. The figures present the induced currents for (a)  $60^\circ$  and (b)  $70^\circ$  designs of the linear array of anomalous reflectors with a  $\lambda/2$  element spacing.

to emphasize that the induced load currents do not remain periodic after performing global optimization because the array is discrete, with a  $\lambda/2$  spacing between the elements.

With 5-bit quantized loads, the scattering patterns closely approach those obtained with continuous load optimization, while increasing the SLL and beam pointing error slightly. With 2- and 3-bit quantized loads, both the SLL and beam pointing error increase notably. The specular reflection rises to or beyond the level in the desired angle. As anticipated, the performance deteriorates significantly with 1-bit load quantization. The discrepancy between the discretized load

outcomes and the continuous loads arises from the constrained degrees of freedom associated with a  $\lambda/2$  spacing. Opting for a more densely arranged configuration will significantly enhance the degrees of freedom for optimizing the induced current distribution, leading to anomalous reflection peaks of higher strengths.

An essential aspect is to assess the efficiency of the antenna scattering synthesis method itself, particularly in terms of the optimization speed. Once the preliminary TX antenna simulations are completed, the multi-objective algebraic optimization process takes less than a minute with 20 distinct loads to obtain the optimal reactive loads, using an HP EliteBook 845 G7 laptop running Windows 10 Enterprise. For reference, a single-objective optimization ignoring the side lobe levels takes only a fraction of a second. Importantly, this technique maximizes the scattering beam in the desired direction, while avoiding full-wave EM simulations within the optimization process.

#### IV. CONCLUSIONS

This paper introduces an efficient design methodology for synthesising finite scattering antenna arrays that enable continuous scanning of reflected beams to arbitrary angles. We have theoretically and computationally shown that a fixed-period linear array can scan into extreme deflection angles with effectively suppressed specular reflection and other parasitic scattering. The method is based on circuit-based algebraic optimization, offering a numerically efficient solution compared with conventional full-wave EM simulation-based optimization approaches (e.g. [11]).

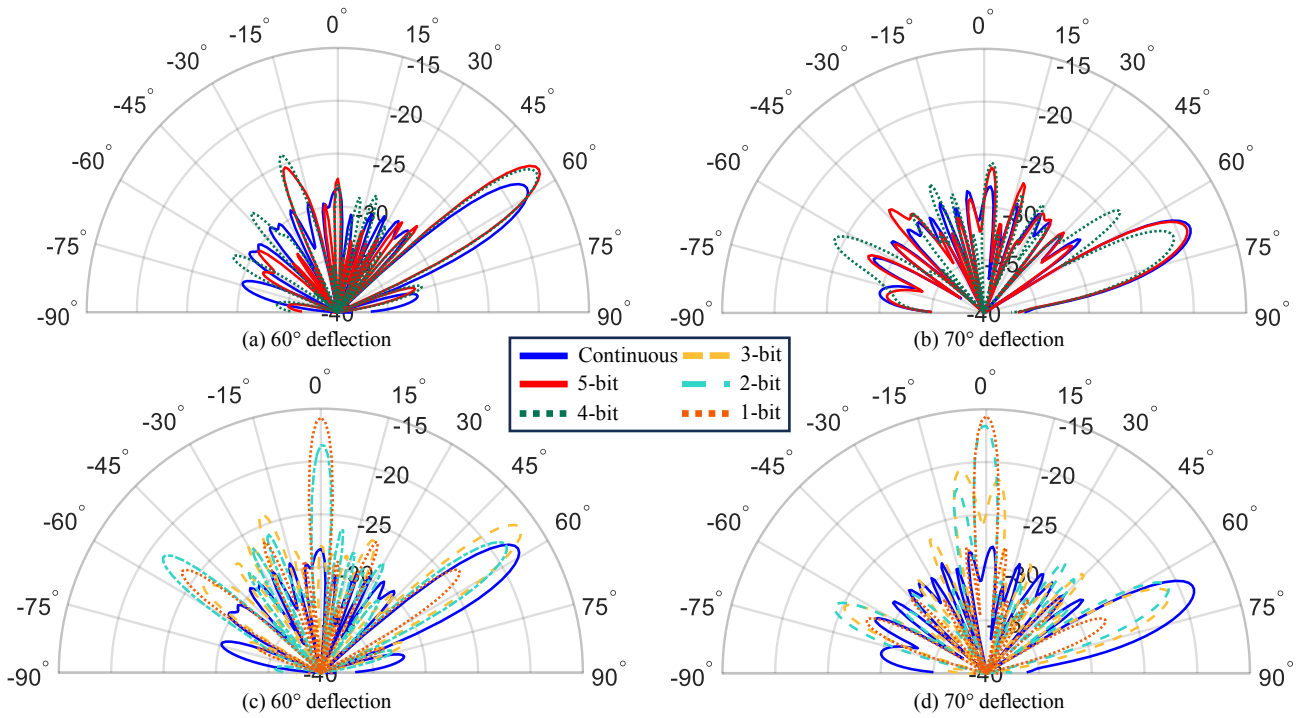


Fig. 5: CST-simulated bistatic SCS patterns (dBsm scale) of the anomalous reflector designs in the  $xz$ -plane, comparing continuous load optimization with discretized loads from 1 to 5-bit quantization resolution. These figures represent the  $xz$ -plane ( $\phi = 0$ ) cut of the bistatic SCS for (a) & (c) 60° and (b) & (d) 70° designs of the linear array of the anomalous reflector with a  $\lambda/2$  element spacing.

The presented studies of arrays with the geometrical period fixed to  $\lambda/2$  show that arrays with properly optimized aperiodically distributed loads have significantly better performance than the conventional phase-gradient reflectarrays. However, we also observe that parasitic scattering is still not eliminated completely. Moreover, in the case of optimizations of only a small set of allowed load reactances (the 1 to 3-bit example), performance degradation is significant.

As is shown in preprint [12], theoretically perfect scanning towards any angle requires a subwavelength spacing between the array elements. In our future work, we will apply the developed algebraic optimization method to arrays with periods less than  $\lambda/2$ , and compare the results with those presented here. Our preliminary results for finite arrays with  $\lambda/4$ -spaced elements are very promising.

#### ACKNOWLEDGMENT

This work received funding from the European Union's Horizon 2020 MSCA-ITN-METAWIRELESS project, under the Marie Skłodowska-Curie grant agreement No 956256, from the Research Council (Academy) of Finland, grant 345178, and the US Army Research Office under grant W911NF-19-2-0244.

#### REFERENCES

- [1] M. Di Renzo, A. Zappone, M. Debbah, M.-S. Alouini, C. Yuen, J. de Rosny, and S. Tretyakov, "Smart radio environments empowered by reconfigurable intelligent surfaces: How it works, state of research, and the road ahead," *IEEE J. Sel. Areas Commun.*, vol. 38, no. 11, pp. 2450–2525, 2020.
- [2] D. Berry, R. Malech, and W. Kennedy, "The reflectarray antenna," *IEEE Trans. Antennas Propag.*, vol. 11, no. 6, pp. 645–651, 1963.
- [3] N. Yu, P. Genevet, M. A. Kats, F. Aieta, J.-P. Tetienne, F. Capasso, and Z. Gaburro, "Light propagation with phase discontinuities: generalized laws of reflection and refraction," *Science*, vol. 334, pp. 333–337, Oct. 2011.
- [4] A. Díaz-Rubio, V. S. Asadchy, A. Elsakka, and S. A. Tretyakov, "From the generalized reflection law to the realization of perfect anomalous reflectors," *Sci. Adv.*, vol. 3, no. 8, p. e1602714, 2017.
- [5] S. K. R. Vuyyuru, R. Valkonen, D.-H. Kwon, and S. A. Tretyakov, "Efficient anomalous reflector design using array antenna scattering synthesis," *IEEE Antennas Wireless Propag. Lett.*, vol. 22, no. 7, pp. 1711–1715, Jul. 2023.
- [6] A. Díaz-Rubio and S. A. Tretyakov, "Macroscopic modeling of anomalously reflecting metasurfaces: Angular response and far-field scattering," *IEEE Trans. Antennas Propag.*, vol. 69, no. 10, pp. 6560–6571, 2021.
- [7] V. Popov, F. Boust, and S. N. Burokur, "Constructing the near field and far field with reactive metagratings: Study on the degrees of freedom," *Phys. Rev. Appl.*, vol. 11, Feb 2019, Art. No. 024074.
- [8] C. A. Balanis, *Antenna Theory: Analysis and Design*. Hoboken, NJ, USA: John Wiley & Sons, 2016.
- [9] R. Collin, "Limitations of the Thevenin and Norton equivalent circuits for a receiving antenna," *IEEE Antennas Propag. Mag.*, vol. 45, no. 2, pp. 119–124, 2003.
- [10] R. C. Hansen, "Relationships between antennas as scatterers and radiators," *Proc. IEEE*, vol. 77, no. 5, pp. 659–662, May 1989.
- [11] V. Popov, B. Ratni, S. N. Burokur, and F. Boust, "Non-local reconfigurable sparse metasurface: Efficient near-field and far-field wavefront manipulations," *Adv. Opt. Mater.*, vol. 9, no. 4, p. 2001316, 2021.
- [12] Y. Li, X. Ma, X. Wang, G. Pitcyn, M. Movahediqomi, and S. A. Tretyakov, "All-angle scanning perfect anomalous reflection by using passive aperiodic gratings," *IEEE Trans. Antennas Propag.*, 2023. [Online]. Available: 10.1109/TAP.2023.3329665